Supplemental Material for

First-principles study of electronic, piezoelectric, optical, and strain-dependent carrier mobility of Janus TiXY (X≠Y, X/Y=Cl, Br, I) monolayers†

Qiu Yang [1], Tian Zhang [2], Cui-E Hu [3,*], Xiang-Rong Chen [1,*], Hua-Yun Geng [4]

[1] Institute of Atomic and Molecular Physics, Sichuan University, Chengdu 610065, China;

[2] College of Physics and Electronic Engineering, Sichuan Normal University, Chengdu 610066, China;

[3] College of Physics and Electronic Engineering, Chongqing Normal University, Chongqing 400047, China;

[4] National Key Laboratory for Shock Wave and Detonation Physics Research, Institute of Fluid Physics, CAEP, Mianyang 621900, China

Abstract:

Janus transition metal dichalcogenide monolayers (TMDs) have attracted wide attention due to their unique physical and chemical properties since the successful synthesis of the MoSSe monolayer. However, the related studies of the Janus monolayers of the transition metal halide (TMHs) type with similar structure are rarely reported. In this paper, we systematically investigated the electronic properties, piezoelectric properties, optical properties, and carrier mobility of the new Janus TiXY (X≠Y, X/Y=Cl, Br, I) from first principles for the first time. The Janus TiXY

* *Corresponding authors. E-mail*: cuiehu@cqnu.edu.cn; xrchen@scu.edu.cn

monolayers are thermally, dynamically, and mechanically stable, and their energy bands near the Fermi level (E_F) are almost entirely contributed by the central Ti atom. Besides, the Janus TiXY monolayers exhibit excellent in-plane and out-of-plane piezoelectric effects, especially for the in-plane piezoelectric coefficient ~ 4.58 pm/V of the TiBrI monolayer and the out-of-plane piezoelectric coefficient ~ 1.63 pm/V of the TiClI monolayer, suggesting their promising applications in the piezoelectric sensors and energy storage. The absorption spectra of the Janus TiXY monolayers are mainly distributed in the visible and infrared regions, implying that they are fantastic candidates in the photoelectric and photovoltaic fields. The calculated results of the carrier mobility revealed that the TiXY monolayers are hole-type semiconductors. Under the regulation of the uniaxial compressive strain, the hole mobilities of these monolayers are gradually improved, indicating that the TiXY monolayers have potential applications in the field of flexible electronic devices.

Keywords: TiXY monolayers; First-principles calculations; Electronic property; Piezoelectric property; Optical property; Carrier mobility

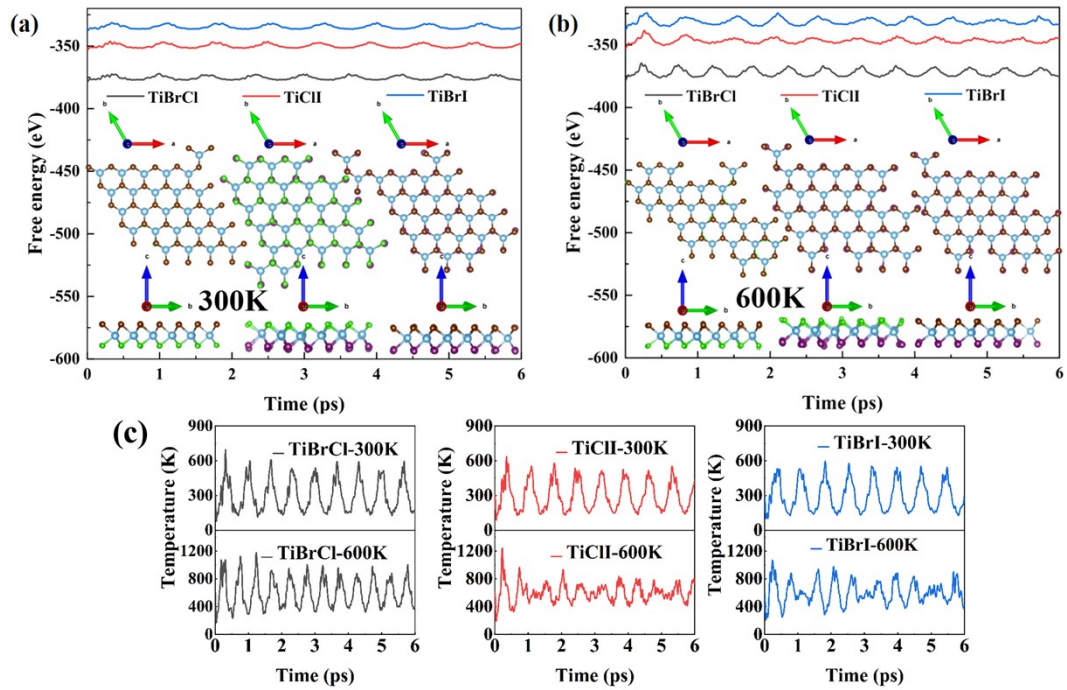

Fig. S1 (Color online) (a) Free energy fluctuations with respect to time and equilibrium structures for Janus TiXY (X≠Y, X/Y=Cl, Br, I) monolayers in AIMD simulations at 300 K; (b) Free energy fluctuations with respect to time and equilibrium structures for Janus TiXY (X≠Y, X/Y=Cl, Br, I) monolayers in AIMD simulations at 600 K; (c) Fluctuation of temperature with time for Janus TiXY (X≠Y, X/Y=Cl, Br, I) monolayers at 300K and 600K cases.

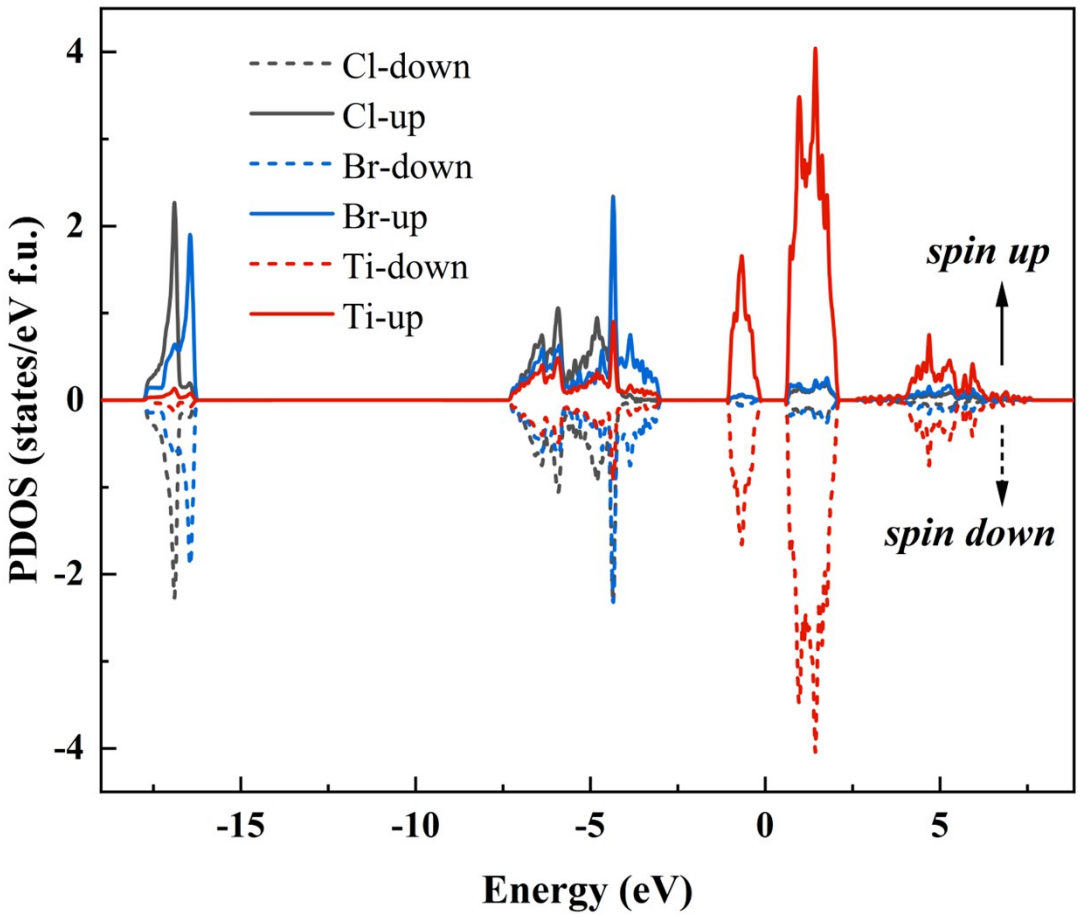

Fig. S2 (Color online) The density of states (DOS) considering spin polarization of the TiBrCl monolayer.

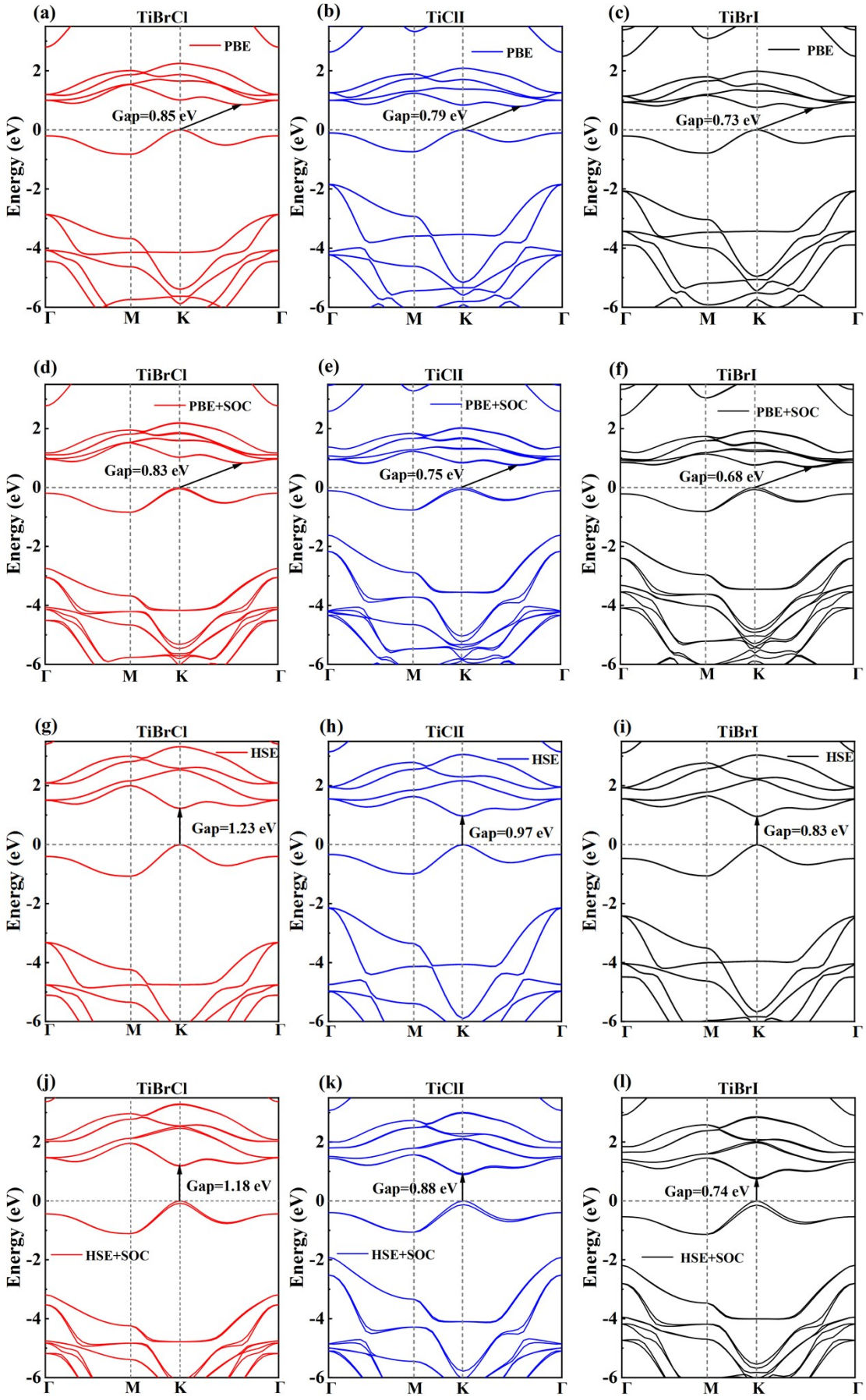
(a)
TiBrCl
PBE
Gap=0.85 eV
(b)
TiClI
PBE
Gap=0.79 eV
(c)
TiBrI
PBE
Gap=0.73 eV
(d)
TiBrCl
PBE+SOC
Gap=0.83 eV
(e)
TiClI
PBE+SOC
Gap=0.75 eV
(f)
TiBrI
PBE+SOC
Gap=0.68 eV
(g)
TiBrCl
HSE
Gap=1.23 eV
(h)
TiClI
HSE
Gap=0.97 eV
(i)
TiBrI
HSE
Gap=0.83 eV
(j)
TiBrCl
Gap=1.18 eV
HSE+SOC
(k)
TiClI
Gap=0.88 eV
HSE+SOC
(l)
TiBrI
Gap=0.74 eV
HSE+SOC
Energy (eV)
Γ M K Γ

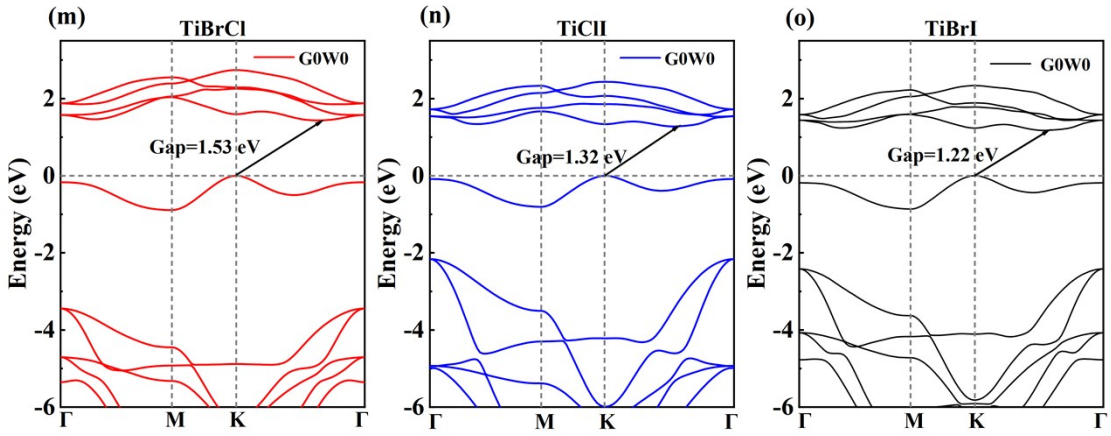

Fig. S3 (Color online) The electronic band structures of the Janus TiXY (X≠Y, X/Y=Cl, Br, I) monolayers. (a), (b), and (c) are the bands calculated by using the PBE method. (d), (e), and (f) are the bands calculated by using the PBE+SOC method. (g), (h), and (i) are the bands computed by using the HSE06 method. (j), (k), and (l) are the bands calculated by using the HSE06+SOC method. (m), (n), and (o) are the bands calculated by using the G_0W_0 method.

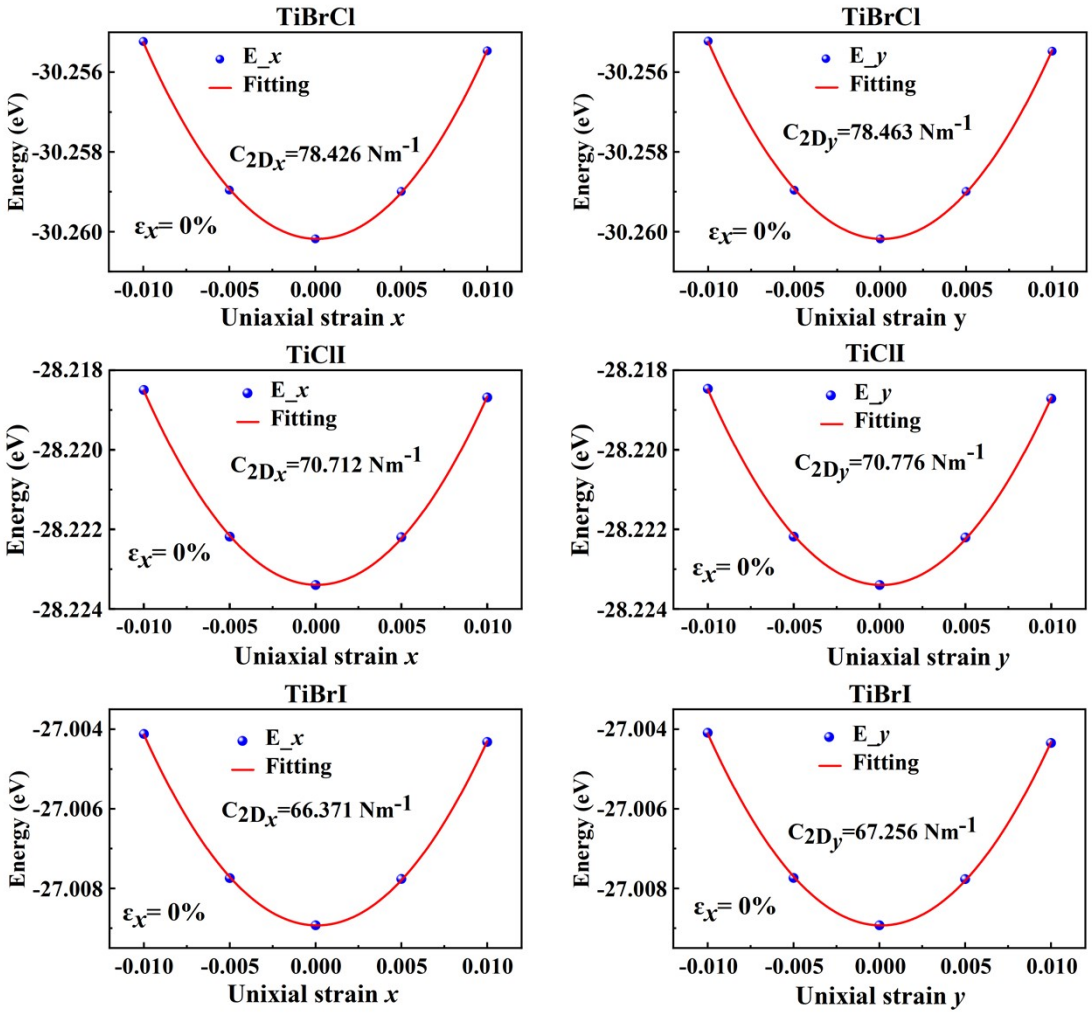

Fig. S4 (Color online) The elastic modulus C_{2D} along the propagation direction is obtained through the quadratic function fitting the total energy of the TiXY monolayers under small uniaxial strain.

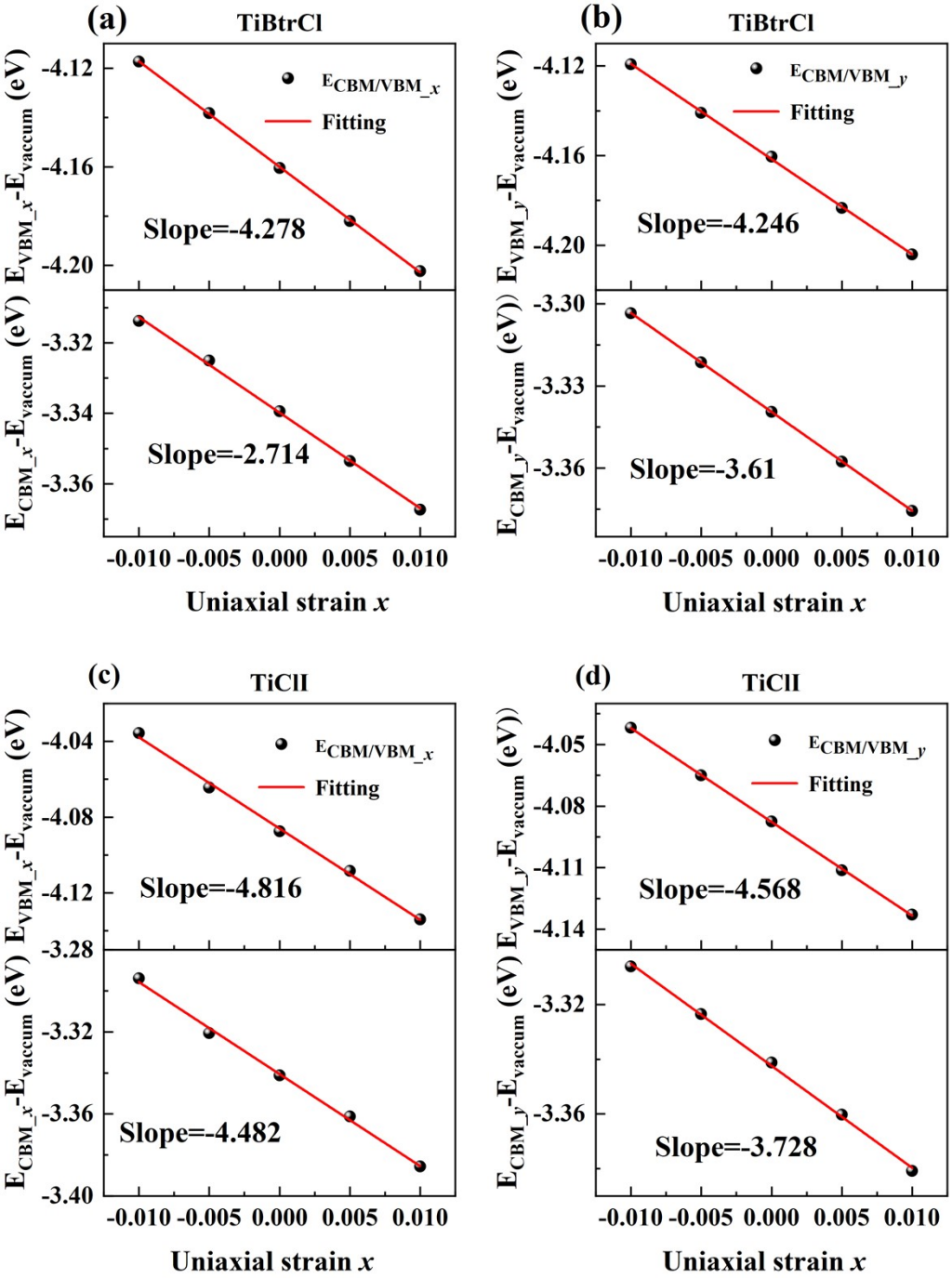
(a)
TiBtrCl
E_CBM/VBM_x
Fitting
Slope=-4.278
Slope=-2.714
E_VBM_x-E_vaccum (eV)
E_CBM_x-E_vaccum (eV)
Uniaxial strain x
(b)
TiBtrCl
E_CBM/VBM_y
Fitting
Slope=-4.246
Slope=-3.61
E_VBM_y-E_vaccum (eV)
E_CBM_y-E_vaccum (eV))
Uniaxial strain x
(c)
TiClI
E_CBM/VBM_x
Fitting
Slope=-4.816
Slope=-4.482
E_VBM_x-E_vaccum (eV)
E_CBM_x-E_vaccum (eV)
Uniaxial strain x
(d)
TiClI
E_CBM/VBM_y
Fitting
Slope=-4.568
Slope=-3.728
E_VBM_y-E_vaccum (eV)
E_CBM_y-E_vaccum (eV))
Uniaxial strain x

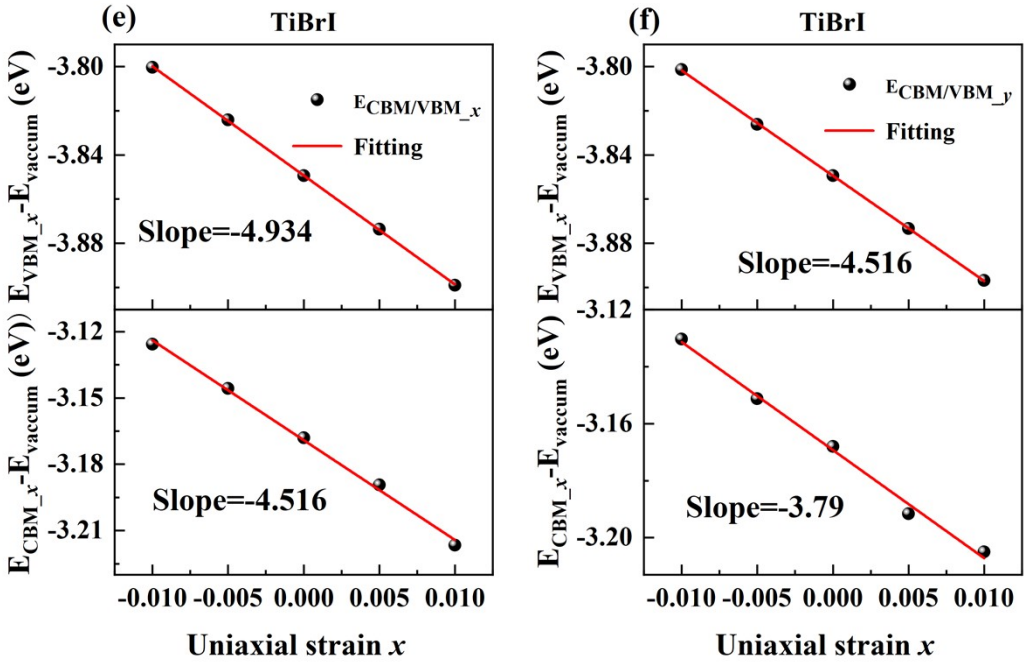

Fig. S5 (Color online) The deformation potential constant E_1 along the propagation direction is obtained by linear fitting the band energies of the VBMs and CBMs with respect to the vacuum energy for the TiXY monolayers.

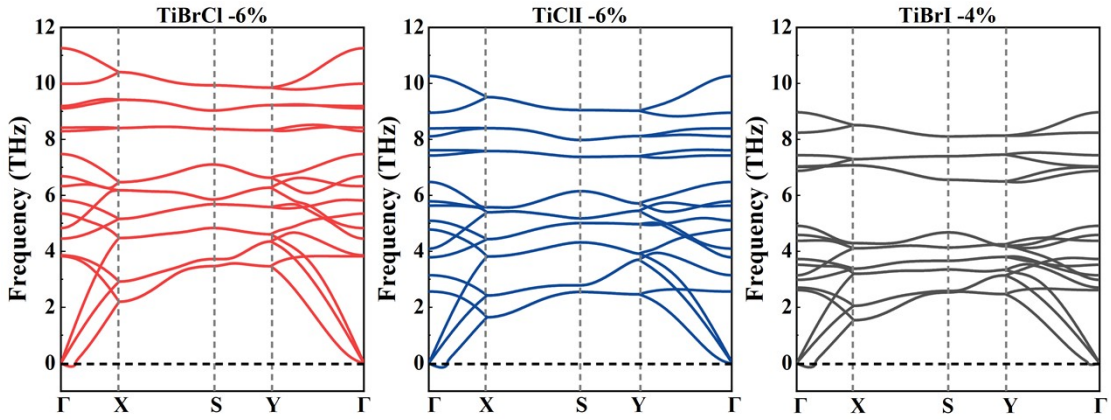

Fig. S6 (Color online) Orthogonal cellular phonon dispersion curves of the compressed structures for the Janus TiXY monolayers: (a) -6% uniaxial strain along *x* direction for TiBrCl; (b) -6% uniaxial strain along *x* direction for TiClI; (c) -4% uniaxial strain along *x* direction for TiBrI.

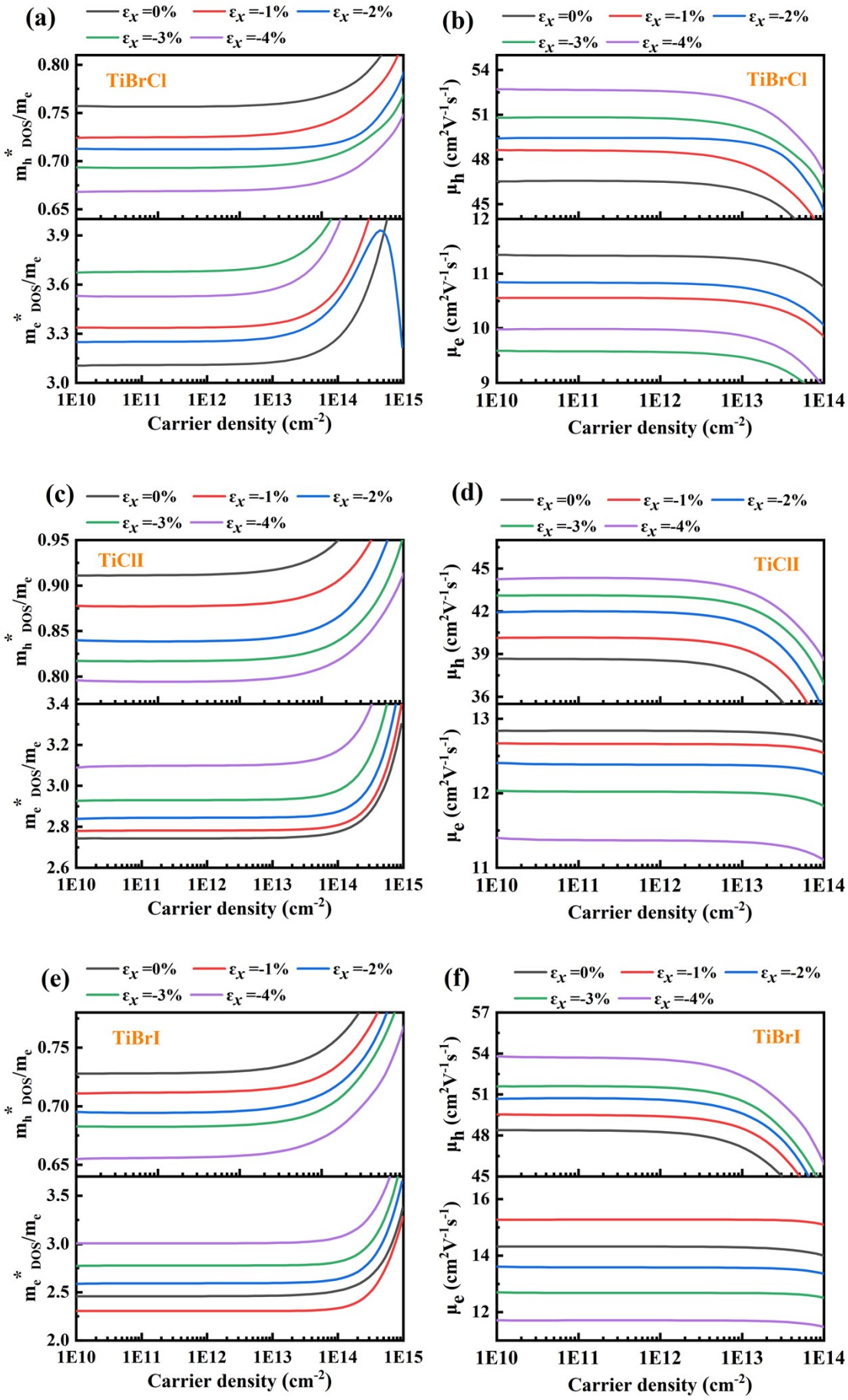
(a)
εx =0%
εx =-1%
εx =-2%
εx =-3%
εx =-4%
TiBrCl
m*h DOS/me
m*e DOS/me
Carrier density (cm-2)
(b)
TiBrCl
μh (cm2V-1s-1)
μe (cm2V-1s-1)
Carrier density (cm-2)
(c)
TiClI
(d)
TiClI
(e)
TiBrI
(f)
TiBrI

Fig. S7 (Color onli1ne) The density-of-states-averaged electron and hole-effective mass $m_{e,h}^{*}(DOS)$ and mobility $\mu_{e,h}$ obtained with the Boltzmann transport theory as a function of the carrier density for monolayer TiBrCl (a), (b); monolayer TiClI (c), (d); and monolayer TiBrI monolayer (e), (f) under different compressive strains ($\varepsilon_x = 0\%, -1\%, -2\%, -3\%, -4\%$). A 10 fs scattering time (τ) was assumed at a constant temperature of 300 K.

Table S1 DOS-averaged effective masses, electrons and mobilities under different uniaxial strains for the Janus TiXY monolayers. These data were calculated at a carrier density of 10^{14} cm^{-2} and the assumption of τ=10 fs.

Materials	Strains	m^{*}_{eD0S} (m_e)	m^{*}_{eD0S} (m_e)	μ^{*}_{eD0S} ($cm^2V^{-1}s^{-1}$)	μ^{*}_{hD0S} ($cm^2V^{-1}s^{-1}$)
TiBrCl	0%	3.106	0.757	11.342	46.523
	-1%	3.337	0.724	10.842	48.632
	-2%	3.248	0.713	10.554	49.421
	-3%	3.676	0.694	9.975	50.785
	-4%	3.528	0.668	9.587	52.714
TiClI	0%	2.744	0.911	12.838	38.665
	-1%	2.781	0.877	12.674	40.127
	-2%	2.843	0.840	12.405	41.955
	-3%	2.929	0.817	12.032	43.117
	-4%	3.097	0.796	11.398	44.295
TiBrI	0%	2.459	0.728	14.325	48.389
	-1%	2.307	0.711	15.264	49.551
	-2%	2.588	0.695	13.614	50.695
	-3%	2.773	0.683	12.702	51.592
	-4%	3.008	0.655	11.711	53.784